Synthesis, characterization, thermal studies, and DFT calculations on Pd(II) complexes containing *N*-methylbenzylamine

Sahra C. Lemos · Silmar J. S. Franchi · Adelino V. G. Netto · Antonio E. Mauro · Oswaldo Treu-Filho · Regina C. G. Frem · Eduardo Tonon de Almeida · Cláudia Torres

Abstract This work describes the synthesis, characterization, and the thermal behavior investigation of four palladium(II) complexes with general formulae $[PdX_2(mba)_2]$, in which mba = *N*-methylbenzylamine and X = OAc^- (**1**), Cl^- (**2**), Br^- (**3**) or I^- (**4**). The complexes were characterized by elemental analysis, infrared vibrational spectroscopy, and ^1H nuclear magnetic resonance. The stoichiometry of the complexes was established by means of elemental analysis and thermogravimetry (TG). TG/DTA curves showed that the thermodecomposition of the four complexes occurred in 3–4 steps, leading to metallic palladium as final residue. The palladium content found in all curves was in agreement with the mass percentages calculated for the complexes. The following thermal stability sequence was found: **3** > **2** > **4** > **1**. The geometry optimization of **1**, **2**, **3**, and **4**, calculated using the DFT/B3LYP method, yielded a slightly distorted square planar environment around the Pd(II) ion made by two anionic groups and two nitrogen atoms from the mba ligand (N1 and N2), in a *trans*-relationship.

Keywords Palladium(II) · *N*-Methylbenzylamine · DFT · TG and DTA

S. C. Lemos · S. J. S. Franchi · A. V. G. Netto (✉) ·
A. E. Mauro · O. Treu-Filho · R. C. G. Frem
Departamento de Química Geral e Inorgânica, Instituto de
Química de Araraquara, UNESP—Univ Estadual Paulista,
P.O. Box 355, Araraquara, SP 14801-970, Brazil
e-mail: adelino@iq.unesp.br

E. T. de Almeida · C. Torres
Departamento de Ciências Exatas, Universidade Federal de
Alfenas, UNIFAL, Alfenas, MG 37130-000, Brazil

Introduction

Cyclopalladated complexes represent an important branch in modern organometallic chemistry since they play important roles not only in organic synthesis [1], photochemistry [2], and homogeneous catalysis [3], but also in the design of liquid crystal materials [4] and new biologically active species [5]. Five-membered palladacycles bearing N-donor organic ligands such as *N*,*N*-dimethylbenzylamine (dmba) and *N*-benzylideneaniline (bzan) as well as halide and pseudohalides as coligands have been one of our major research interests [6–8]. This class of compounds exhibits promising antimycobacterial and antitumoral activities [9–11], interesting supramolecular assemblies in solid state [12], and a plethora of reactivity such as 1,3-dipolar cycloaddition of multiply bonded molecules [13, 14] and insertion reactions of acetylenes into Pd–C bond [15].

During our attempts to prepare cyclometallated complexes from the reaction between *N*-methylbenzylamine (mba) and palladium(II) acetate (Fuchita's synthesis [16]), we have obtained analytical and spectroscopic evidences of the formation of coordination compounds of the type $[PdX_2(mba)_2]$, in which X = OAc^- (**1**), Cl^- (**2**), Br^- (**3**), I^- (**4**). In pursuing our interest in the coordination chemistry [17–20], biological activity [21, 22], and thermal behavior [23–27] of transition metal compounds containing N-based ligands, we present herein the synthesis, characterization, DFT calculations, and thermal studies on compounds **1**–**4** (Scheme 1) by means of thermogravimetry (TG) and differential thermal analysis (DTA).
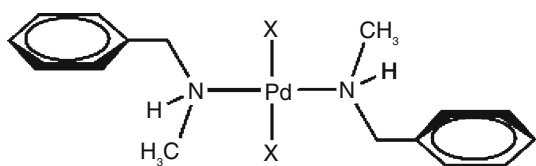
Experimental

General comments

All reagents were obtained from commercial suppliers and used without further purification.

Scheme 1 Structural representation of the compounds [PdX$_2$(mba)$_2$] (X = OAc$^-$ (**1**), Cl$^-$ (**2**), Br$^-$ (**3**), I$^-$ (**4**))

Synthesis of the complexes

Complex **1** was prepared as follows: 4.91 mmol (595 mg) of *N*-methylbenzylamine were added to a suspension of [Pd(OAc)$_2$] (4.44 mmol, 995.6 mg) in 50 mL of benzene. The mixture was stirred at 60 °C for 1 day. The resulting yellow suspension was filtered off. The solid material was washed with benzene and dried under vacuum. Yield: 77%. Compounds **2–4** were readily obtained by metathetical reactions of [Pd(OAc)$_2$(mba)$_2$] with the appropriate amount of KX salts in a mixture of methanol:acetone (2:1). The resulting suspensions were filtered off and the solids were washed and dried under vacuum. Yield 62–87%.

Instrumentation

Elemental analyses of carbon, nitrogen, and hydrogen were performed on a microanalyser elemental analyser CHN, model 1112 FLASH EA. Infrared spectra were recorded in KBr pellets on a Nicolet model SX-FT-Impact 400 spectrophotometer in the 4000–400 cm^{-1} spectral range. ^{1}H NMR spectra were recorded in CDCl$_3$ solutions at room temperature on a Varian INOVA 500 spectrometer. Melting points were determined on a MAPFQ apparatus. Thermal analyses (TG) and differential thermal analyses (DTA) were carried out using a TA *Instruments* model SDQ 600, under flow of dry synthetic air (50 mL min^{-1}), temperature up to 900 °C and at heating rate of 20 °C min^{-1} in α-alumina sample holders. The reference substance was pure α-alumina in DTA measurements. X-ray powder diffraction patterns were measured on a Siemens D-5000 X-ray diffractometer using Cu K$_\alpha$ radiation ($\lambda = 1.541$ Å) and setting of 34 kV and 20 mA. The peaks were identified using ICDD bases [28].

Computational strategy

In this work, the employed quantum chemical approach to determining the molecular structures was Becke three-parameter hybrid theory [29] using the Lee–Yang–Par (LYP) correlation functional [30] and the basis sets used for calculations were: [4s] for H (^{2}S) [31], [5s4p] for C (^{3}P), N (^{4}S), and O(^{3}P) [31], [11s7p] for Cl (^{2}P) [32],

[16s9p5d] for I (^{2}P),[1] and [12s8p5d] for Pd (^{1}S) [31]. In order to better describe the properties of **1–4** in the implementation of the calculations, it was necessary to include polarization functions for all atoms of the compounds. The strategy to choice of the polarization functions was previously described [31]. The polarization functions are: $\alpha_p = 0.33353749$ for H (^{2}S), $\alpha_d = 0.72760279$, and $\alpha_d = 0.35416230$ for C (^{3}P) and N (^{4}S), respectively, and $\alpha_f = 0.14057699$ for Pd (^{1}S) atoms [31]. For Cl atom (^{2}P), the polarization function to the basis set previously reported [32] is $\alpha_d = 0.47236655$. The polarization function for Br (^{2}P) and I atoms (^{2}P) are reported in this work: is $\alpha_f = 0.42912802$ for Br (see footnote [1]) and $\alpha_f = 0.51068618$ for I.[2] We undertook a computed geometry optimization using the optimized algorithm of Berny [33]. The performed molecular calculations in this work were done using the Gaussian 09 routine [34]. The principal infrared-active fundamental modes assignments and descriptions were done by the GaussView W 5.0.8 graphics routine [35].

Results and discussion

The elemental analysis and thermogravimetric results together with IR spectroscopy and ^{1}H NMR data confirmed the proposed formulae for the complexes **1–4**. Table 1 represents the colors, melting points and the results of elemental analysis.

Infrared spectra

Table 2 represents some selected absorptions of the IR spectra of the complexes along with their assignments. The overall pattern of the IR spectra of **1–4** resembles very closely to that of the free ligand. The coordination of

---

[1] Basis set for Br (^{2}P) atom. The 27s19p12d [discretization parameters: $\Omega_{(s)} = -0.455$, $\Delta\Omega_{(s)} = 0.123$, N$_{(s)} = 6.0$; $\Omega_{(p)} = -0.388$, $\Delta\Omega_{(p)} = 0.110$, N$_{(p)} = 6.0$; $\Omega_{(d)} = -0.265$, $\Delta\Omega_{(d)} = 0.124$, N$_{(d)} = 6.0$]/15s11p6d (10,4,1,1,1,1,1,1,1,1,1,1,1,1,1,1/9,1,1,1,1,1,1,1,1,1,1,1/7,1,1,1,1,1) basis set were built with the add of the Generator Coordinate Hartree–Fock method. The polarization function is $\alpha_f = 0.42912802$. Full details about the wave function developed in this work for sulfur are available upon request to the e-mail address: oswatreu@iq.unesp.br.

[2] Basis set for I (^{2}P) atom. The 31s22p16d [discretization parameters: $\Omega_{(s)} = -0.417$, $\Delta\Omega_{(s)} = 0.112$, N$_{(s)} = 6.0$; $\Omega_{(p)} = -0.492$, $\Delta\Omega_{(p)} = 0.112$, N$_{(p)} = 6.0$; $\Omega_{(d)} = -0.219$, $\Delta\Omega_{(d)} = 0.107$, N$_{(d)} = 6.0$]/16s9p5d (8,7,1,1,1,1,1,1,1,1,1,3,3,1,1,1,1,1/8,1,1,1,1,3,3,3,1/10,1,3,1,1) basis set were built with the add of the Generator Coordinate Hartree–Fock method. The polarization function is $\alpha_f = 0.51068618$. Full details about the wave function developed in this work for sulfur are available upon request to the e-mail address: oswatreu@iq.unesp.br

Table 1 Results of elemental analyses and melting points of the compounds **1**–**4**

Complex	Color	M.p./°C	Found (calcd.)/%		
			C	H	N
$C_{20}H_{28}N_2O_4Pd$ (**1**)	Yellow	129	51.9 (51.5)	5.9 (6.1)	6.3 (6.0)
$C_{16}H_{22}N_2Cl_2Pd$ (**2**)	Yellow	170	45.5 (45.8)	5.5 (5.3)	6.6 (6.7)
$C_{16}H_{22}N_2Br_2Pd$ (**3**)	Yellow	154	37.9 (37.8)	4.7 (4.4)	5.5 (5.7)
$C_{16}H_{22}N_2I_2Pd$ (**4**)	Orange	155	32.2 (31.9)	3.6 (3.7)	4.7 (4.7)

N-methylbenzylamine by the nitrogen atom in **1**–**4** was evidenced by the appearance of the typical absorptions of the –NHCH$_3$ moiety at ∼3200 (νNH), 2920 (ν_{as}CH$_3$), and 2862 cm^{-1} (ν_sCH$_3$). The shift of the absorption band attributed to the δNH + δCH$_3$ mode to lower frequency (ca. 1052 cm^{-1}) when compared with that one of the free ligand (1103 cm^{-1}) is also indicative of coordination. In addition, two out-of-plane C–H bending vibrational modes (γCH) were observed as very intense bands at 750 and 700 cm^{-1} which strongly supports the presence of monosubstituted phenyl rings. The ν_{as}COO$^-$ and ν_sCOO$^-$ vibrational modes for coordinated acetate groups in **1** appeared as two broadened and intense absorptions over the spectral range of 1650–1350 cm^{-1}, respectively. The νPd–X and νPd–N band frequencies are expected to occur below 350 cm^{-1} [36]. However, the νPd–X and νPd–N absorptions could not be detected since the spectrophotometer used in this work operates in the 4000–400 cm^{-1} range.
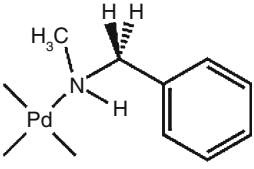
^{1}H NMR spectra

The observed chemical shifts in the ^{1}H NMR spectra of *N*-methylbenzylamine and the complexes are shown in Table 3.

The ^{1}H NMR spectra of **1**–**4** showed that the *N*-methylbenzylamine is coordinated to the metallic center by the nitrogen atom due to the downfield shift of NH signals from 1.35 ppm (mba ligand) to 2.42–3.48 ppm. In addition, the methylene group attached to NH in the complexes **1**–**4** appeared as multiplets whereas in the ^{1}H NMR spectrum of mba a singlet was noticed at 3.69 ppm. The observed loss of magnetic equivalence of methylene groups the ^{1}H NMR spectra of the complexes clearly indicates the coordination of mba.

The analytical and IR results obtained for compounds **1**–**4** suggest a square planar environment around the Pd atom whose coordination sites are occupied by two nitrogen atoms from mba ligands, and two anionic X$^-$ groups (X$^-$ = Cl, Br, I, OAc). The *trans*-configuration was attributed to these complexes on basis of known X-ray structures of similar compounds of general formulae *trans*-[PdX$_2$L$_2$] {L = N-based ligands; X$^-$ = Cl [37], Br [38], I [39], OAc [40]}. As no single crystal for X-ray diffraction studies could be obtained, the structures of the Pd(II) compounds **1**–**4** were optimized using DFT theory (B3LYP method) and are shown in Fig. 1. A selection of calculated bond lengths and angles is shown in Table 4.

The calculated structures for **1**–**4** show a satisfactory agreement with the available crystal structure data of similar compounds of the type [PdX$_2$L$_2$] (L = N-based ligands) [37–40], mainly in terms of bond lengths. The calculations of vibrational frequencies were employed to determine whether optimized geometries constitute

Table 2 Selected experimental (exp) and calculated (calc) IR frequencies (cm^{-1}) together with percentual error (p.e.) for complexes **1**–**4**

Assignment	Wavenumber/cm^{-1}											
	1			**2**			**3**			**4**		
	exp	calc	p.e.	exp	calc	p.e.	exp	calc	p.e.	exp	calc	p.e.
νNH	3178	3100	−2.5	3221	3391	+5.3	3198	3382	+5.7	3178	3375	+6.2
νCH$_{ring}$	3049	3181	+4.3	3032	3172	+4.6	3026	3172	+4.8	3049	3171	+4.0
νCH$_3$	2920	3097	+6.0	2921	3106	+6.3	2914	3028	+3.9	2920	3032	+3.8
ν_{as}COO	1630	1613	−1.0	–	–	–	–	–	–	–	–	–
ν_{ring}	a	1532	–	1495	1487	−0.5	1491	1488	−0.6	1491	1488	−0.2
δCH$_2$	a	1379	–	1423	1377	−3.2	1421	1377	−3.1	1454	1385	−4.7
δCH$_3$ + ν_sCOO	1315	1350	+2.7	–	–	–	–	–	–	–	–	–
νCN + γCH	908	891	−1.9	910	881	−3.2	905	880	−2.8	905	876	−3.2
γCH$_{ring}$	748	760	+1.6	746	767	+2.8	748	765	+2.3	748	768	+2.7
γCH$_{ring}$	a	716	–	698	716	+2.6	702	716	+2.0	696	723	+3.9
δOCO	688	681	−1.0	–	–	–	–	–	–	–	–	–

^{a} Obscured

Table 3 ¹H NMR data (ppm) for compounds **1–4** at 298 K, in CDCl₃-*d* given as δ (ppm), multiplicity [integration]

Scheme		¹H NMR data			
		NH	–CH₂–	N–CH₃	–C₆H₅
	mba	ᵃ	3.69 s, [2H]	2.40 s, [3H]	7.20–7.27 m, [5H]
	1	ᵃ	3.14–3.09 m, [1H]	2.12 s, [3H]	7.42–7.25 m, [5H]
			3.90–3.85 m, [1H]		
	2	3.38 s, [1H]	3.47–3.51 m, [1H]	2.43 s, [3H]	7.36–7.43 m, [5H]
			4.21–4.25 m, [1H]		
	3	3.39 al, [1H]	3.50–3.58 m, [1H]	2.47–2,42 m, [3H]	7.36–7.42 m, [5H]
			4.21–4.28 m, [1H]		
	4	3.40 al, [1H]	3.44–3.49 m, [1H]	2.45 s, [3H]	7.40–7.48 m, [5H]
			4.01–4.07 m, [1H]		

s singlet, *m* multiplet

ᵃ Not observed

Fig. 1 Calculated structures of *trans*-[PdX₂(mba)₂] (X = OAc⁻ (**1**), Cl⁻ (**2**), Br⁻ (**3**), I⁻ (**4**))
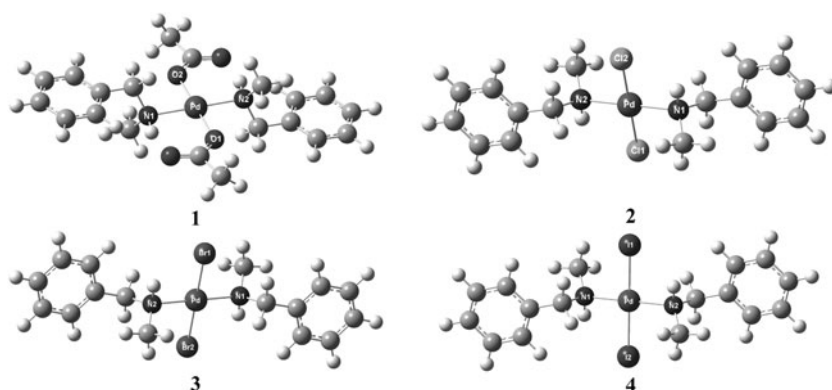
Table 4 Selected calculated bond lengths (Å), and bond angles (°) for **1**, **2**, **3**, and **4**

[Pd(OAc)₂(mba)₂] (**1**)		[PdCl₂(mba)₂] (**2**)		[PdBr₂(mba)₂] (**3**)		[PdI₂(mba)₂] (**4**)	
Bond lengths/Å							
Pd–N1	2.11213	Pd–N1	2.10607	Pd–N1	2.11459	Pd–N1	2.11469
Pd–N2	2.11261	Pd–N2	2.10603	Pd–N2	2.11448	Pd–N2	2.11470
Pd–O1	2.07235	Pd–Cl1	2.38488	Pd–Br1	2.50963	Pd–I1	2.59335
Pd–O2	2.07217	Pd–Cl2	2.38499	Pd–Br2	2.50974	Pd–I2	2.59329
Bond angles/°							
N1–Pd–O1	84.932	N2–Pd–Cl2	93.718	N2–Pd–Br2	93.740	N2–Pd–I2	94.253
O1–Pd–N2	95.020	Cl2–Pd–N1	86.273	Br2–Pd–N1	86.256	I2–Pd–N1	85.758
N2–Pd–O2	84.947	Cl1–Pd–N1	93.725	Br1–Pd–N1	93.745	I1–Pd–N1	94.231
O2–Pd–N1	95.100	Cl1–Pd–N2	86.284	Br1–Pd–N2	86.260	I1–Pd–N2	85.757
O1–Pd–O2	179.962	Cl1–Pd–Cl2	179.970	Br1–Pd–Br2	179.945	I1–Pd–I2	179.989
N1–Pd–N2	179.940	N1–Pd–N2	179.982	N1–Pd–N2	179.977	N1–Pd–N2	179.975

minimum or saddle points. The most important theoretical frequencies values calculated for the compounds are also depicted in Table 2. The calculated frequencies are in good agreement with the experimental values, with a percentual error less than 6%, supporting the suggested *trans*-[PdX₂(mba)₂] structure.

Thermogravimetric analysis

TG and DTA curves obtained for the compounds **1–4** are shown in Fig. 2 and Table 5 lists the results of the thermal studies of these compounds together with the assignments of each decomposition stage based on mass calculation.

Fig. 2 TG and DTA curves of the complexes [PdX$_2$(mba)$_2$] (X = OAc$^-$ (**1**), Cl$^-$ (**2**), Br$^-$ (**3**), I$^-$ (**4**))
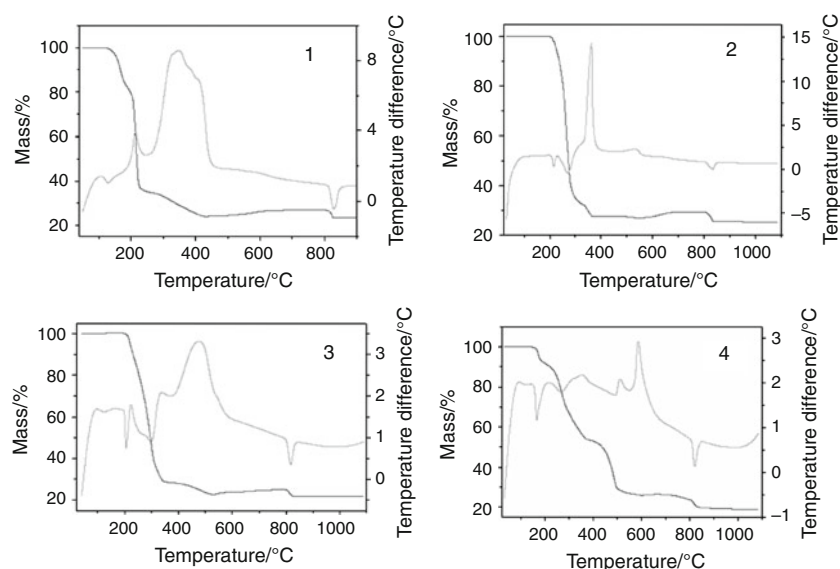

Table 5 Thermal analysis data for compounds [PdX$_2$(mba)$_2$] (X = OAc$^-$ (**1**), Cl$^-$ (**2**), Br$^-$ (**3**), I$^-$ (**4**))

Complex	Step	ΔT/°C	Δm/%	DTA peak/°C	
				Endo	Exo
1	1	111–421	−75.71	125.3	213; 251–468
	2	421–813	+2.42	–	–
	3	813–829	−3.21	828	–
	Residue		23.50	–	–
2	1	189–365	−72.53	214; 269	362
	2	365–799	+1.86	–	532
	3	799–842	−3.93	833	–
	Residue		25.40	–	–
3	1	197–355	−71.29	204; 224–337	–
	2	355–529	−5.95	–	476
	3	529–789	+2.30	–	–
	4	789–832	−3.07	817	–
	Residue		21.99	–	–
4	1	134–368	−45.89	164; 265	352
	2	368–612	−28.15	–	511; 585
	3	612–809	−2.73	–	–
	4	809–875	−3.70	822	–
	Residue		19.53	–	–

Therefore, the groups indicated at the right column of Table 2 do not correspond necessarily to the gaseous final products of decomposition. The X-ray powder diffractograms of the final products, obtained after the decomposition of PdO, showed the characteristic peaks of Pd (ASTM 05-0681).

Complex **1** and **2** present similar decomposition patterns. The first step of decomposition corresponds to the release of organic and inorganic ligands together with uptake of O$_2$, leading to the partial conversion of Pd to PdO. In complex **1** this step occurs in the range 111–421 °C and is accompanied by one endothermic peak at 125 °C in the DTA curve and two exothermic signals at 213 °C and 251–468 °C. In the second step there is an increase in mass of 2.42% which is attributed to the uptake of O$_2$ and conversion of the remaining Pd to PdO. This process is completed at 813 °C. The third and final step corresponds to the decomposition of PdO to Pd, which finishes at 829 °C and is accompanied by an endothermic peak at 828 °C in the DTA curve. This behavior was already observed for other palladium complexes [21].

For the complex **2**, the first step of decomposition occurs in the range 189–365 °C, accompanied by two endothermic peaks at 214 and 269 °C and one exothermic signal at 362 °C. This mass variation is ascribed, by mass calculations, to the release of organic and inorganic ligands and partial conversion of Pd to PdO. The second step (365–799 °C) is attributed to an increase in mass of 1.86%, related to the uptake of O$_2$ and conversion of the remaining Pd to PdO. This process is related to the exothermic peak at 532 °C in the DTA curve. The third step is completed at 842 °C and corresponds to the decomposition of PdO to Pd which is associated with the endothermic peak at 828 °C.

The decomposition of complex **3** occurs in four steps. The release of organic and inorganic ligands together with uptake of O$_2$ occurs in the two initial steps: 197–355 and 355–529 °C. These events are accomplished by endothermic signals at 204 and 224–337 °C and by an exothermic peak at 476 °C in the DTA curves. The final residue of the second step consists of a mixture of Pd and PdO. The third step (529–789 °C) corresponds to the uptake of O$_2$ and conversion of the remaining Pd to PdO. The last mass loss is characterized by the decomposition of PdO to Pd and is

completed at 832 °C (endothermic peak in the DTA curve at 817 °C).

Complex **4** displays a different thermal decomposition pattern. TG curve of compound **4** shows two consecutive mass loss in the range 134–368 °C assigned, by mass calculation, to the loss of one organic ligand unit (mba) and one iodide. This process is related to the endothermic peaks at 164 and 265 °C and one exothermic peak at 352 °C. The following steps are overlapped: a mass loss at 368–612 °C, followed by a slight mass increase over the range 612–669 °C and a final mass decrease which is completed at 809 °C. Due to the complexity of the decomposition, the assignments of these steps could not be done by mass calculations. A further increase of temperature to 879 °C results in the last mass loss which is ascribed to the reduction of PdO to Pd. The palladium content found in the decomposition is in agreement with the mass percentage calculated for the complex.

Taking into account the initial decomposition temperatures, the thermal stability of the complexes [PdX$_2$(mba)$_2$] varies in the sequence: X = **3** > **2** > **4** > **1**. The thermodecomposition of the complex [Pd(OAc)$_2$(mba)$_2$] (**1**) initiates at the lowest temperature among all the complexes studied. The low thermal stability of complex **1** was already expected in agreement with our previous results [8]. On the other hand, bromo- and chloro-derivatives exhibit the highest thermal stability.

Conclusions

Synthesis, characterization, and thermal behavior of four [PdX$_2$(mba)$_2$] type complexes in which mba = *N*-methylbenzylamine and X = OAC$^-$ (**1**), Cl$^-$ (**2**), Br$^-$ (**3**), and I$^-$ (**4**), were investigated in this work. IR and ^{1}H NMR spectra indicated that in the four complexes the organic ligand is coordinated to the metal by the nitrogen atom in a neutral monodentate mode. Taking into account the initial decomposition temperatures, the following thermal stability sequence could be established: **3** > **2** > **4** > **1**. The thermogravimetric data showed that all decompositions initiate with the release of organic and inorganic ligands, followed by the uptake of O$_2$, leading to the formation of a mixture of Pd and PdO. Afterwards, all PdO is decomposed to Pd^0, which is the final residue of the thermal decomposition of **1**–**4**. The computational strategy used in this work represents a good alternative for calculations on vibrational frequencies of metal-based compounds.

References

1. La Deda M, Ghedini M, Aiello I, Pugliese T, Barigelletti F, Accorsi G. Organometallic emitting dyes: palladium(II) nile red complexes. J Organomet Chem. 2005;690:857–61.
2. Yasuike S, Okajima S, Yamaguchi K, Seki H, Kurita J. New optically active organoantimony (BINASb) and bismuth (BINABi) compounds comprising a 1,1′-binaphtyl core: synthesis and their use in transition metal-catalysed asymmetric hydolysation of ketones. Tetrahedron. 2003;59:4959–66.
3. Kurzeev SA, Kazankov GM, Ryabov AD. Increased catalytic activity of primary amine palladacycles in biomimetic hydrolysis of *N*-t-*BOC*-*S*-methionine *p*-nitrophenyl ester. Inorg Chim Acta. 2000;305:1–6.
4. Díez L, Espinet P, Miguel JA, Rodríguez-Medina MP. Mesogens based on plalladium orthometallated complexes with carboxylato bridges: tuning and shaping a non-planar molecule. J Organomet Chem. 2005;690:261–8.
5. Caires ACF, de Almeida ET, Mauro AE, Hemerly JP, Valentini SR. Síntese e atividade citotóxica de alguns azido-ciclopaladados estabilizados com ligantes bifosfínicos. Quim Nova. 1999;22:329–34.
6. Tomita K, Caires ACF, Neto VAD, Mauro AE. Structure of a cyclopalladated complex, [PdCl(C$_{37}$H$_{32}$N)]. Acta Cryst C. 1994;50:1872–3.
7. Stevanato A, Mauro AE, Netto AVG. Thermal spectroscopic investigation on N N-dimethylbenzylamine based cyclopalladated compounds containing isonicotinamide. J Therm Anal Calorim. 2009;97:149–52.
8. de Almeida ET, Santana AM, Netto AVG, Torres C, Mauro AE. Thermal study of cyclopalladated complexes of the type [Pd$_2$(dmba)$_2$X$_2$(bpe)]. J Therm Anal Calorim. 2005;82:361–4.
9. Moro AC, Mauro AE, Netto AVG, Ananias SR, Quilles MB, Carlos IZ, Pavan FR, Leite CQF, Hörner M. Antitumor and antimycobacterial activities of cyclopalladated complexes: X-ray structure of [Pd(C2, N-dmba)(Br)(tu)] (dmba = N, N-dimethylbenzylamine, tu = thiourea). Eur J Med Chem. 2009;44:4611–5.
10. Rocha MC, Santana AM, Ananias SR, de Almeida ET, Mauro AE, Placeres MCP, Carlos IZ. Citotoxicity and immune response induced by organopalladium(II) in mice bearing Ehrlich ascites tumor. J Braz Chem Soc. 2007;18:1473–80.
11. de Almeida ET, Mauro AE, Santana AM, Netto AVG. Emprego de compostos organometálicos mononucleares de paládio(II) na ativação de macrófagos peritoneais de camundongos. Quim Nova. 2005;28:405–8.
12. de Almeida ET, Mauro AE, Santana AM, Ananias SR, Netto AVG, Ferreira JG, Santos RHA. Self-assembly of organometallic Pd(II) complexes via CH$_3$ π interactions: the first example of a cyclopalladated compound with herringbone stacking pattern. Inorg Chem Commun. 2007;10:1394–8.
13. Mauro AE, Caires ACF, Santos RHD, Gambardella MTD. Cycloaddition reaction of the azido-bridged cyclometallated complex [Pd(dmba)N$_3$]$_2$ with CS$_2$. Crystal and molecular structure of di(μ-N, S-1,2,3,4,-thiatriazole-5-thiolate)bis[N,N-dimethylbenzyl-amine-C2, N)palladium(II)]. J Coord Chem. 1999;48:521–8.
14. Santana AM, Mauro AE, Almeida ET, Netto AVG, Klein SI, Santos RHA, Zoia JR. 1,3-Diploar cycloaddition of CS$_2$ to the coordination azide in the cyclopalladated [Pd(bzan)(μ-N$_3$)]$_2$. Crystal and molecular structure of di(μ-N, S-1,2,3,4-thiatrizole-5-thiolate)bis[(benzylideneaniline-C2, N)palladium(II)]. J Coord Chem. 2001;53:163–72.
15. Ananias SR, Santana AM, Mauro AE, Neto VAL, de Almeida ET. Reação de bis-inserção de 1,2-difenilacetileno na ligação Pd–C de ciclometalados. Quim Nova. 2003;26:53–5.

16. Fuchita Y, Tsuchiya H, Miyafuji A. Cyclopalladation of secondary and primary benzylamines. Inorg Chim Acta. 1995;233:91–6.

17. Legendre AO, Mauro AE, Ferreira JG, Ananias SR, Santos RHA, Netto AVG. A 2D coordination polymer with brick-wall network topology based on the [Cu(NCS)$_2$(pn)] monomer. Inorg Chem Commun. 2007;10:815–20.

18. Netto AVG, Frem RCG, Mauro AE. Low-weight coordination polymers derived from the self-assembly reactions of Pd(II) pyrazolyl compounds and azide ion. Polyhedron. 2005;24:1086–92.

19. Netto AVG, Frem RCG, Mauro AE. Synthesis and spectroscopic characterization of a novel coordination polymer of palladium(II) with pyrazole and azido ligands. Mol Cryst Liq Cryst. 2002;374:255–60.

20. Netto AVG, Mauro AE, Frem RCG, Santana AM, Santos RHA, Zoia JR. Synthesis and structural characterization of dichlorobis(1-phenyl-3-methylpyrazole)palladium(II) and diazidobis(1-phenyl-3-methylpyrazole)palladium(II). J Coord Chem. 2001;54:129–41.

21. Rocha FV, Barra CV, Netto AVG, Mauro AE, Carlos IZ, Frem RCG, Ananias SR, Quilles MB, Stevanato A, Rocha MC. 3,5-Dimethyl-1-thiocarbamoylpyrazole and its Pd(II) complexes: synthesis, spectral studies and antitumor activity. Eur J Med Chem. 2010;45:1698–702.

22. de Souza RA, Stevanato A, Treu-Filho O, Netto AVG, Mauro AE, Castellano EE, Carlos IZ, Pavan FR, Leite CQF. Antimycobacterial and antitumor activities of palladium(II) complexes containing isonicotinamide (isn): X-ray structure of trans-[Pd(N$_3$)$_2$(isn)$_2$]. Eur J Med Chem. 2010;45:4863–8.

23. Netto AVG, Takahashi PM, Frem RCG, Mauro AE, Zorel Júnior HE. Thermal decomposition of palladium(II) pyrazolyl complexes. Part I. J Anal Appl Pyrolysis. 2004;72:183–9.

24. Netto AVG, Santana AM, Mauro AE, Frem RCG, de Almeida ET, Crespi MS, Zorel Júnior HE. Thermal decomposition of palladium(II) pyrazolyl complexes. Part II. J Therm Anal Calorim. 2005;79:339–42.

25. Netto AVG, Frem RCG, Mauro AE, Crespi MS, Zorel Júnior HE. Synthesis, spectral and thermal studies on pyrazolate-bridged palladium(II) coordination polymers. J Therm Anal Calorim. 2007;87:789–92.

26. Fernandes RL, Takahashi PM, Frem RCG, Netto AVG, Mauro AE, Matos JR. Synthesis, spectral and thermal studies on dicarboxylate-bridged palladium(II) coordination polymers. Part I. J Therm Anal Calorim. 2009;97:123–6.

27. Fernandes RL, Takahashi PM, Frem RCG, Netto AVG, Mauro AE, Matos JR. Synthesis, spectral and thermal studies on dicarboxylate-bridged palladium(II) coordination polymers. Part II. J Therm Anal Calorim. 2009;97:153–6.

28. Powder diffraction file of the Joint Committee on Powder Diffraction Standards. Sets 1-32, published by the International Center of Diffraction Data, Swarthmore, PA 19081, USA (1982).

29. Becke AD. Density-functional thermochemistry III. The role of exact exchange. J Chem Phys. 1993;98:5648–52.

30. Lee C, Yang W, Parr RG. Development of the Colle–Salvetti correlation energy formula into a functional of the energy density. Phys Rev B. 1988;37:785–9.

31. Treu-Filho O, Pinheiro JC, da Costa EB, Ferreira JEV, de Figueiredo AF, Kondo RT, de Lucca Neto VA, de Souza RA, Legendre AO, Mauro AE. Experimental and theoretical study of the compound [Pd(dmba)(NCO)(imz)]. J Mol Struct. 2007;829:195–201.

32. Treu-Filho O, Pinheiro JC, de Souza RA, Kondo RT, Ferreira RDP, de Figueiredo AF, Mauro AE. Molecular structures and vibrational frequencies for cis-[PdCl$_2$(tmen)] and cis-[Pd(N$_3$)$_2$(tmen)]: a DFT study. Inorg Chem Commun. 2007;100:1501–4.

33. Li X, Frisch MJ. Energy-represented DIIS within a hybrid geometry optimization method. J Chem Theory Comput. 2006;2:835–9.

34. Frisch MJ, Trucks GW, Schlegel HB, Scuseria GE, Robb MA, Cheeseman JR, Scalmani G, Barone V, Mennucci B, Petersson GA, Nakatsuji H, Caricato M, Li X, Hratchian HP, Izmaylov AF, Bloino J, Zheng G, Sonnenberg JL, Hada M, Ehara M, Toyota K, Fukuda R, Hasegawa J, Ishida M, Nakajima T, Honda Y, Kitao O, Nakai H, Vreven T, Montgomery Jr. JA, Peralta JE, Ogliaro F, Bearpark M, Heyd JJ, Brothers E, Kudin KN, Staroverov VN, Kobayashi R, Normand J, Raghavachari K, Rendell A, Burant JC, Iyengar SS, Tomasi J, Cossi M, Rega N, Millam JM, Klene M, Knox JE, Cross JB, Bakken V, Adamo C, Jaramillo J, Gomperts R, Stratmann RE, Yazyev O, Austin AJ, Cammi R, Pomelli C, Ochterski JW, Martin RL, Morokuma K, Zakrzewski VG, Voth GA, Salvador P, Dannenberg JJ, Dapprich S, Daniels AD, Farkas O, Foresman JB, Ortiz JV, Cioslowski J, Fox DJ, Gaussian 09, Revision A.02. Wallingford, CT: Gaussian, Inc.; 2009.

35. GaussView 5.0.8: Copyright (c) 2000–2008 Semichem, Inc.

36. Nakamoto K. Infrared and Raman spectra for inorganic and coordination compounds. Part B: applications in coordination, organometallic, and bioinorganic chemistry. 5th ed. New York: Wiley-Interscience Publication; 1997.

37. Sui-Seng C, Zargarian D. trans-Bis(benzylamine)dichloropalladium(II). Acta Cryst E. 2003; E59:m957–8.

38. Clifford SE, Tiwow V, Gendron A, Maeder M, Rossignoli M, Lawrance GA, Turner P, Blake AJ, Schröder M. Complexation of constrained ligands piperazine, N-substituted piperazines, and thiomorpholine. Aust J Chem. 2009;62:1196–206.

39. Ha K. Crystal structure of diiodobis(acridine)palladium(II), PdI$_2$(C$_{13}$H$_9$N)$_2$. Z. Kristallogr. NCS. 2010;225:693–4.

40. Halligudi SB, Bhatt KN, Khan NH, Kurashy RI, Venkatsubramanian K. Synthesis, structural characterization and catalytic carbonylation of nitrobenzene and amines by mononuclear palladium(II) complexes containing substituted pyridine ligands. Polyhedron. 1996;15:2093–101.